Agrisera
Part of Thermo Fisher Scientific

This product is **for research use only** (not for diagnostic or therapeutic use) **contact: support@agrisera.com**

Agrisera AB | Box 57 | SE-91121 Vännäs | Sweden | +46 (0)935 33 000 | www.agrisera.com

Product no AS13 2640

Anti-ACT | Actin (polyclonal)

Product information

Immunogen	ca. 100 amino acids of recombinant actin conserved more than 80% in *Arabidopsis thaliana:* actin-1 P0CJ46 AT2G37620, actin-2 Q96292 AT3G18780, actin-3 P0CJ47 AT3G53750, actin-4 P53494 AT5G59370, actin-5 Q8RYC2 At2g42100, actin-7 P53492 At5g09810, actin-8 Q96293 AT1G49240 , actin-11 P53496 , AT3G12110 ,actin-12 P53497 AT3G46520
Host	Rabbit
Clonality	Polyclonal
Purity	Serum
Format	Lyophilized
Quantity	50 µl
Reconstitution	For reconstitution, add 50 µl of sterile water
Storage	Store lyophilized/reconstituted at -20°C; once reconstituted make aliquots to avoid repeated freeze-thaw cycles. Please remember to spin the tubes briefly prior to opening them to avoid any losses that might occur from material adhering to the cap or sides of the tube.
Additional information	Antibody available in 3 various pack sizes: 50, 100 and 150 µl - Please inquire. This product can be sold containing ProClin if requested.

Application information

Recommended dilution	1: 250 (ExM), 1-100 - 1 : 250 (IF), 1 : 3000-1 : 5000 (WB)
Expected | apparent MW	41.6 | 45 kDa
Confirmed reactivity	*Actinidia* sp., *Agostis stolonifera*cv. 'Penncross', *Arabidopsis thaliana, Brassica* napus, *Cucumis sativus, Cyanthobasis fruticulosa, Cynara cardunculus, Fragaria x ananassa,, Glycine max, Hordeum vulgare, Mentha spicata, Nicotiana tabacum, Odontarrhena lesbiaca, Petrosimonia nigdeensis, Phaseolus vulgaris, Phaeodactylum tricornutum, Phoenix dactylifera, Picrorhiza kurroa, Prunus avium, Salsola grandis, Salsola tragus, Setaria italica, Solanum tuberosum, Triticum aestivum, Vigna unguiculata, Vitis vinifera, Zea mays*
Predicted reactivity	*Agropyron cristatum, Beta vulgaris, Betula luminifera, Brassica rapa subsp. pekinensis, Daucus carota, Cannabis sativa* L. *, Capsella rubella,¨Capsicum annuum, Castanea sativa, Chorispora bungeana, Cyanidioschyzon merolae strain 10D, Glycine soja, Halogeton glomeratus, Helianthus annuus, Ipomoea batatas, Manihot esculenta, Medicago truncatula, Malus domestica, Oryza sativa, Pisum sativun, Populus sp., Saccharum officinarum, Solanum lycopersicum, Solanum tuberosum, Phaeodactylum tricornutum, Picea abies, Picea sitchensis, Prunus avium, Olea europaea, Ricinus communis, Rubus plicatus, Theobroma cacao, Trebouxia* sp., *Vicia faba* Species of your interest not listed? Contact us
Not reactive in	*Chlamydomonas reinhardtii* (too high background for this species)
Selected references	Wilkinson et al. (2026). Nat Commun. 2026 Mar 27;17(1):2883. doi: 10.1038/s41467-026-71012-y. AUXIN RESPONSE FACTOR thermostability. D'Agostino et al. (2026). Gallic Acid- Responsive microRNAs Reprogram Lignification During Drought Acclimation Process in Spearmint. Plant Biotechnol J . 2026 Mar 14. doi: 10.1111/pbi.70599. Telara et al. (2026). Hypoxic and Fe-Responses are Regulated by the ERFVII Factors and the PCO Branch of the N-Degron Pathway According to Iron Availability.Plant Cell Environ. 2026 Mar 8. doi: 10.1111/pce.70466. Yang et al. (2026). GmAP1 delays flowering time and confers sensitivity to salt stress in soybean. Plant Physiology and Biochemistry Volume 232, March 2026, 111163. Holzner et al. (2026). The chloroplast ionome shines light on the dynamics of organellar iron homeostasis. Plant Cell. 2026 Jan 29:koag017. doi: 10.1093/plcell/koag017. Piechowiak et al. (2025), Ozone Treatment Enhances Antioxidant Status and Energy Metabolism in Radish (Raphanus sativus) Sprouts. Springer Nature, Food Bioprocess Technology. Titeli et al. (2025). Transcription factors PaWRKY57 and PaNAC29 regulate fruit color and growth during sweet cherry development. Plant Physiol. 2025 Dec 13:kiaf647. doi: 10.1093/plphys/kiaf647. Kocacinar et aL. (2025). Biochemical and structural differences between C3 cotyledons and C4 leaves in species of Salsoloideae (Chenopodiaceae). Sci Rep. 2025 Oct 17;15(1):36383.doi: 10.1038/s41598-025-20388-w. Xiao et al. (2025). A fungal effector promotes infection via stabilizing a negative regulatory factor of chloroplast immunity. Nat Commun. 2025 Jul 29;16(1):6970. doi: 10.1038/s41467-025-62326-4. Ling et al. (2025). Natural variation of AcEGY3 mediates chloroplastic ROS homeostasis to confer kiwifruit thermotolerance. Nat Commun. 2025 Jul 4;16(1):6184.doi: 10.1038/s41467-025-61593-5.

Sportès et al. (2025). A transcriptomic perspective of P trade in mycorrhizal grapevine. Mycorrhiza. 2025 May 28;35(3):39.doi: 10.1007/s00572-025-01200-z.
Cox Jr et al. (2025). ExPOSE: a comprehensive toolkit to perform expansion microscopy in plant protoplast systems. The Plant Journal, Volume121, Issue 5, doi.org/10.1111/tpj.70049.
Uflewski et al. (2024). The thylakoid proton antiporter KEA3 regulates photosynthesis in response to the chloroplast energy status. Nat Commun. 2024 Mar 30;15(1):2792. doi: 10.1038/s41467-024-47151-5.
Lorrai et al. (2024). Cell wall integrity modulates HOOKLESS1 and PHYTOCHROME INTERACTING FACTOR4 expression controlling apical hook formation. Plant Physiol. 2024 Jul 8:kiae370. doi: 10.1093/plphys/kiae370.
Salesse-Smith et al. (2024). Greater mesophyll conductance and leaf photosynthesis in the field through modified cell wall porosity and thickness via AtCGR3 expression in tobacco. Plant Biotechnol J. 2024 Apr 30.doi: 10.1111/pbi.14364.

Ciesielska et al. (2024). S2P2-the chloroplast-located intramembrane protease and its impact on the stoichiometry and functioning of the photosynthetic apparatus of A. thaliana. Front Plant Sci. 2024 Mar 15:15:1372318. doi: 10.3389/fpls.2024.1372318.
Pavlovič et al. (2024). Diethyl ether anaesthesia inhibits de-etiolation of barley seedlings by locking them in intermediate skoto-photomorphogenetic state. Physiol Plantarum, Volume176, Issue 1.
Soria et al. (2024).Functional resilience: An active oxidative phosphorylation system prevails amid foreign proteins in holoparasitic plants. Current Plant Biology Volume 37, March 2024, 100322.
Blagojevic et al. (2024). Heat stress promotes Arabidopsis AGO1 phase separation and association with stress granule components. iScience. 2024 Feb 6;27(3):109151. doi: 10.1016/j.isci.2024.109151. eCollection 2024 Mar 15.
Gong et al. (2024). HYPK controls stability and catalytic activity of the N-terminal acetyltransferase A in Arabidopsis thaliana. Cell Rep. 2024 Feb 15;43(2):113768.doi: 10.1016/j.celrep.2024.113768.

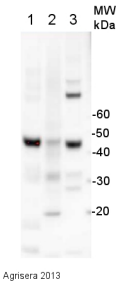

15 µg of total protein extracted with PEB (**AS08 300**) from leaf tissue of (**1**) *Arabidopsis thaliana*, (**2**) *Hordeum vulgare*, (**3**) *Zea mays* were separated on **4-12%** NuPage (Invitrogen) **LDS-PAGE** and blotted 1h to **PVDF**. Filters were blocked 1h with 2% low-fat **milk powder** in TBS-T (0.1% TWEEN 20) and probed with **anti-actin** (AS13 2640, **1:2500**, 1h) and secondary anti-rabbit (**1:10 000**, 1 h) antibody (HRP conjugated, recommended secondary antibody AS09 602) in TBS-T containing 2% low fat milk powder. Antibody incubations were followed by washings in TBS-T (15, +5, +5, +5 min). All steps were performed at RT with agitation. Signal was detected with chemiluminescent detection reagent using a Fuji LAS-3000 CCD (300s, standard sensitivity). Exposure time was 2 min.

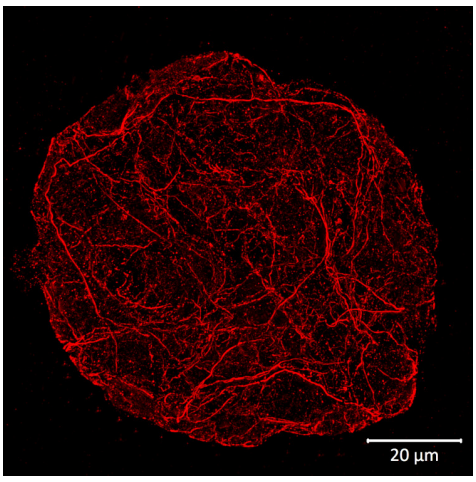

Type of material: isolated plant protoplasts from *Arabidopsis thaliana* wild type
Fixation: formaldehyde | Methanol, 37°C | 3.2 % paraformaldehyde in W5 buffer (150 mM NaCl, 125 mM $CaCl_2$, 5 mM KCl, 2 mM MES pH 5.7), fixed overnight at +4ºC Hydrophilization: no
Cell wall digestion: yes
Membrane permeabilization: DMSO-IGEPA
Antigen retrieval: no
Blocking buffer: 2% BSA in 1X Phosphate Buffered Saline (PBS) buffer pH 7.2
Washing buffer: after primary antibody incubation 3 washes were done with 2% BSA in 1X PBS buffer, after secondary antibody incubation – with 1X PBS buffer
Primary antibody dilution and incubation time: 1:250 in blocking buffer, incubation was done overnight at +4ºC
Secondary antibody dilution and incubation time and supplier: anti-rabbit antibody conjugated with DyLight™ 594 (AS12 2076, Agrisera), diluted in a blocking buffer to a final concentration of 1:500.
Incubation time: 3 hours at room temperature on a shaker.
Co-staining of the nucleus (DAPI): no
Cell wall and nucleus staining: no

Details of the ExM (Expansion microscopy method) on A. thaliana and *Zea mays* protoplasts are described here.

Courtesy Dr. Kirk Czymmek, The Donald Danforth Plant Science Center, USA

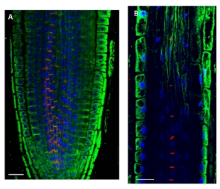

Actin cytoskeleton in 5 days old *Arabidopsis thaliana* seedlings. Actin signal shown in green, PIN1 in red and DAPI in blue. The material has been fixed in 2 % formaldehyde for 45 minutes. Tissue cleaning has been performed before immunolocalization. Rabbit anti-actin primary antibody was diluted in 1:250 and anti-rabbit Alexa 488 and Alexa 555 were both diluted in 1: 500 (Invitrogen). Scale bar - 20 µm.

Courtesy: Dr. Taras Pasternak, Freiburg University, Germany

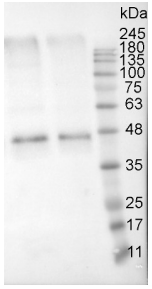

Proteins were extracted from tuber flesh of Russet Burbank potato (*Solanum tuberosum*) with 0.1 M Tris HCl (pH=8.0), 5% sucrose (m/v), 2% (m/v) SDS, protease inhibitors (PMSF 1mM). Samples were heated 95°C 5 min, and 10 µg of total protein was resolved in 12% SDS PAGE and blotted to PVDF membrane for 1h-1.5h using tank transfer. Blots were blocked with a skimmed milk 4% (m/v) in T-TBS (1.5h) at RT with agitation. Primary antibodies (AS13 2640) were applied overnight +4°C in dilution 1:5000 with agitation. After washing with T-TBS 2-3 times, membrane was incubated with secondary antibodies (Goat Anti-Rabbit HRP conjugate, Transgen biotech HS101) 1:10000 for 1 hour at RT. Blot was washed as above and developed with ECL (Clarity Western ECL Substrate, BioRad, 170-5060) for 5 – 10 minutes. Exposure time – 20.395 seconds.

Courtesy of Iauhenia Isayenka, University of Sherbrooke, Canada